

Fig. 1. Micellar formation and characterization of SMA/CORM2. (A) Diagrammatic illustration of SMA/CORM2 micelle structure. (B) The hydrodynamic size of SMA/CORM2 micelles in aqueous solution determined via dynamic light scattering (DLS). (C) TEM of SMA/CORM2 micelles. (D) Summary of the physicochemical characteristics of SMA/CORM2 micelles. The size as measured by TEM is that of one unit cell of micelles. When 2–4 units are clustered in water, the micelle size agrees well with that found by DLS.

revealed a spherical SMA/CORM2 appearance; most unit micelles had diameters of 30–80 nm, but two or three particles tended to cluster together, and thus the molecules appeared larger, more than 100 nm (Fig. 1C). These findings suggested that SMA/CORM2 self-associated to form supramolecular structures in aqueous medium. In addition, it is interesting that SMA/CORM2 micelles in PBS(–) exhibited a much weaker zeta potential (–13.5 mV) compared with that of free SMA (–50 mV).

To determine the CORM2 loading in SMA/CORM2 micelles, we performed elemental analysis of the ruthenium (ICP-AES) in CORM2. The content of ruthenium in SMA/CORM2 micelles was 4.1% (w/w) when CORM2 and SMA were applied at the ratio of 1:5 (g/g). CORM2 loading in the micelles was thus calculated to be ~11% according to chemical structure, and the total yield was 66.7% based on CORM2 (Fig. 1D). The resultant SMA/CORM2 showed good water solubility (>50 mg/ml in a physiological water solution). In addition, when the feed ratio of CORM2 to SMA was increased to 1:3, the resultant compounds were difficult to dissolve in water (data not shown), which indicated that high loading of CORM2 may lead to insufficient coverage of the hydrophobic core and thus a reduced water solubility.

3.2. Profiles of CO release from SMA/CORM2

We then used CO-detecting gas chromatography to measure the velocity of CO release from SMA/CORM2 and compared it with that of the parental CORM2. As expected, parental CORM2 in the DMSO solution demonstrated a very rapid CO release rate, i.e. almost all CO was released within 10–30 min (data not shown), whereas SMA/CORM2 in PBS(–) solution manifested a much slower CO release (e.g. <5%/day) (Fig. 2A). Complete release of CO from SMA/CORM2, within 1 h, was

observed for SMA/CORM2 in the DMSO solution (Fig. 2A), because the micelles were completely disrupted in the solvent. These findings indicated the effects of solvents on the stability of the micelles and the CO release properties of SMA/CORM2. Furthermore, when a surfactant (Tween 20 or saponin) was added to an aqueous solution of SMA/CORM2, the micelle structure disintegrated, the surfactant thus facilitating CO release (Fig. 2A). Incubation of SMA/CORM2 in saponin for 24 h resulted in an almost complete release of CO (Fig. 2A), so saponin was used as the CO-releasing agent in our *in vivo* pharmacokinetic study, as described below. More important, when lecithin, the major component of cell membranes, was added to the SMA/CORM2 solution, CO release was also increased (Fig. 2A), which suggests that SMA/CORM2 micelles may be disrupted during the intracellular uptake process and subsequently release CO. Similar results were observed for other SMA micelles in our laboratory [22,25].

CO release from SMA/CORM2 was also examined at different pH values. As Fig. 2B illustrates, for the range of pH 2 to 10, no significant increase in CO release was found for up to 48 h. This result suggested a pH stability of SMA/CORM2 as well as the possibility of oral administration of SMA/CORM2.

More importantly, we measured the release of CO from SMA/CORM2 in the presence of 100% fetal bovine serum to mimic the *in vivo* behavior of SMA/CORM2 (Fig. 2C). Compared with free CORM2, which reached a peak CO release in 30 min, SMA/CORM2 had a slower and more sustained CO release, which gradually increased in 24 h and lasted up to 48–72 h. We thus expected that SMA/CORM2 would show superior *in vivo* pharmacokinetics compared with the parent CORM2, which would guarantee improved bioavailability of CO after systemic administration of SMA/CORM2. We therefore performed a pharmacokinetic study, as described below.

3.3. *In vivo* pharmacokinetics of SMA/CORM2

We first determined the CO concentration in circulation after *i.v.* injection of SMA/CORM2 or free CORM2 in normal BALB/c mice. Because most CO exists in circulation as CO-hemoglobin, we used the NO-releasing agent NOC7 to purge hemoglobin-bound CO. Fig. 3A shows that the CO concentration in the blood of healthy BALB/c mice was about 10 nM. Administration of free CORM2 induced a prompt increase in CO (to a 3.5-fold higher value) in circulating blood at 2 h, followed by a decrease in CO because of its removal from the lung through respiration; the CO concentration was about twice that of the basal level after 24 h (Fig. 3A). Similar to the results seen in Fig. 2C, CO in circulation demonstrated a much slower and constant increase after *i.v.* SMA/CORM2 administration. The CO concentration increased to 3.7 times that of the basal level and was maintained at relatively high levels for up to 48 h (Fig. 3A). In addition, when SMA/CORM2 was administered orally, prolonged high CO concentration in circulation, similar to those after *i.v.* administration, was also observed (Supplemental Fig. S3A). These findings suggested that superior *in vivo* bioavailability of CO could be achieved by SMA/CORM2 compared with free CORM2.

We then investigated the *in vivo* pharmacokinetics of SMA/CORM2 by using saponin to liberate all the CO in circulation, including CO bound to hemoglobin as well as CO from injected SMA/CORM2, as described in Section 2.4.2. We calculated the CO from the SMA/CORM2 that remained in circulation by subtracting hemoglobin-bound CO from total CO quantified by means of the saponin method, and we analyzed the results to evaluate the *in vivo* pharmacokinetics. As seen in Fig. 3B and Table 1, after *i.v.* injection SMA/CORM2 exhibited a 35-fold longer blood $t_{1/2}$ (21.2 h) compared with free CORM2 (0.6 h). Moreover, the area under the concentration vs. time curve of SMA/CORM2 was about 17 times greater than that of free CORM2, and the body clearance of SMA/CORM2 was about 16 times slower than that of free CORM2 (Table 1).

In addition, when administered orally, blood concentration of SMA/CORM2 continuously increased to 2 h after which it gradually

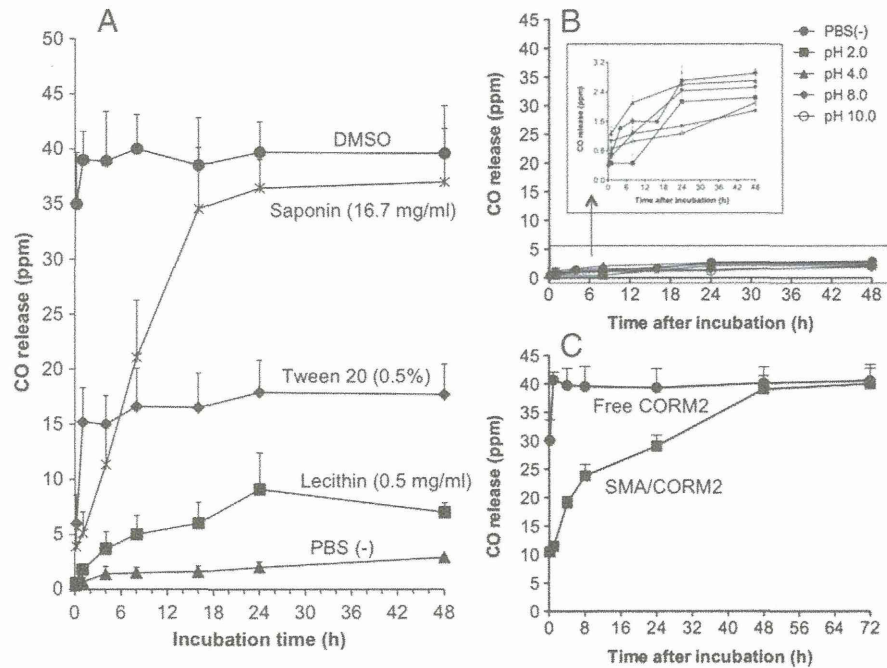


Fig. 2. Release of CO from SMA/CORM2 micelles. (A) SMA/CORM2 was dissolved in different solutions, and CO released from SMA/CORM2 was quantified at different time points by using gas chromatography. (B) The influence of pH on CO release. The data showed little effect of a pH shift on CO release. (C) CO release profiles were also determined in the presence of 100% fetal bovine serum. The concentration of SMA/CORM2 used in this study was 4 mg/ml (equivalent to 0.4 mg/ml CORM2), and 1 ml of each sample was analyzed. For the experiment of free CORM2 shown in (C), it was first dissolved in DMSO at 4 mg/ml, then 0.1 ml of this solution was added into 0.9 ml of 100% fetal bovine serum. Data are means \pm SD; $n = 3-6$. See text for details.

decreased, at 24 h and 48 h the blood concentrations were at the same levels of those after i.v. injection (Supplemental Fig. S3B).

These findings are consistent with general observations about macromolecular drugs and polymer therapeutics. For example, compared with conventional small molecule drugs, large molecules including polymer conjugates, micelles, and nanoparticles usually show significantly prolonged circulation times because their size prevents renal clearance. Support for this idea comes from many examples, not only from laboratory research but also from clinical experiences with such drugs as pegylated interferon and others [12–15,26]. We thus believe that clinical development of SMA/CORM2 is possible.

More importantly, the major advantage of macromolecular drugs is their disease-targeted delivery. As opposed to normal tissues, tumor tissues and inflammatory tissues demonstrate unique pathophysiological characteristics, e.g. highly active angiogenesis and enhanced vascular permeability because of overproduction of many vascular mediators including bradykinin, NO, and vascular endothelial growth factors. Macromolecular drugs larger than 40–50 kDa (the renal threshold) will thus extravasate into and accumulate in diseased tissues but will show less distribution in normal tissues because of reduced extravasation from normal blood vessels [12–15].

The term coined for this phenomenon is the ERP effect. It is now an important standard in the design and development of drugs, especially anticancer drugs [12–15,26,27]. Because of the EPR effect, SMA/CORM2, which is a polymer micelle with a prolonged circulation time as described above (Fig. 3A, Table 1), may accumulate selectively in pathological lesions. To verify this interpretation, we utilized a murine colitis model and investigated the tissue distribution of SMA/CORM2 after its i.v. administration. The total CO liberated by saponin was used to estimate the behavior of SMA/CORM2 and free CORM2. After i.v. injection of SMA/CORM2, the results, which agreed well with the expectation as based on the EPR effect, showed a significantly greater CO increase (9 times higher) in colitis tissues compared with that for free CORM2, and high CO levels continued for at least 24 h, with the peak at 4 h (Fig. 3C). Similar results were also found when SMA/CORM2 was given by oral route though the peak levels of CO was lower

(Supplemental Fig. S3C). Furthermore, at 4 h after i.v. injection of SMA/CORM2, the CO concentration in colitis tissues was significantly higher than that in normal colon and in most normal organs including the kidney, lung, and heart but not the liver and spleen (Fig. 3D). The distribution in the liver and spleen was probably due to capture of the polymer micelles by the rich reticuloendothelial system in the liver and spleen; similar phenomena were observed for many other polymeric drugs and nanoparticles [15,28,29]. However, because both liver and spleen are rich in heme proteins, the CO in those organs may also derive partly from those proteins during circulation.

On the basis of the findings described above, we found superior *in vivo* pharmacokinetics of SMA/CORM2 compared with pharmacokinetics of free CORM2 (Fig. 3B, C, D), which resulted from the EPR effect. The prolonged circulation time and selective accumulation of SMA/CORM2 in diseased tissues led to greatly improved CO bioavailability, which suggests that SMA/CORM2 have many advantages as a CO donor in the treatment of inflammatory diseases. We therefore investigated the therapeutic potential of SMA/CORM2 in a murine colitis model, as described below.

3.4. *In vivo* therapeutic effect of SMA/CORM2 on DSS-induced murine colitis

In this investigation, we studied both systemic (i.v. injection) and oral administration of SMA/CORM2. Because of the good pH stability of SMA/CORM2 over a wide pH range (Fig. 2B), we expected that the micelles would not be rapidly destroyed in the stomach and that they may thus reach colitis lesions and have a local therapeutic effect.

In this DSS-induced colitis model, the colitis group that had no SMA/CORM2 treatment manifested severe diarrhea accompanied by hematochezia at day 7, as indicated by the increased DAI values (Fig. 4A), along with the decrease in body weight (Fig. 4B). Diarrhea markedly improved with SMA/CORM2 given either by i.v. injection or oral administration. The SMA/CORM2 treatment groups had significantly lower DAI values during the experimental period and manifested no apparent loss of body weight compared with normal animals (Fig. 4A and B). Moreover, the colon was significantly shortened, which is an index of colitis, in mice with DSS-induced colitis (Fig. 4C),

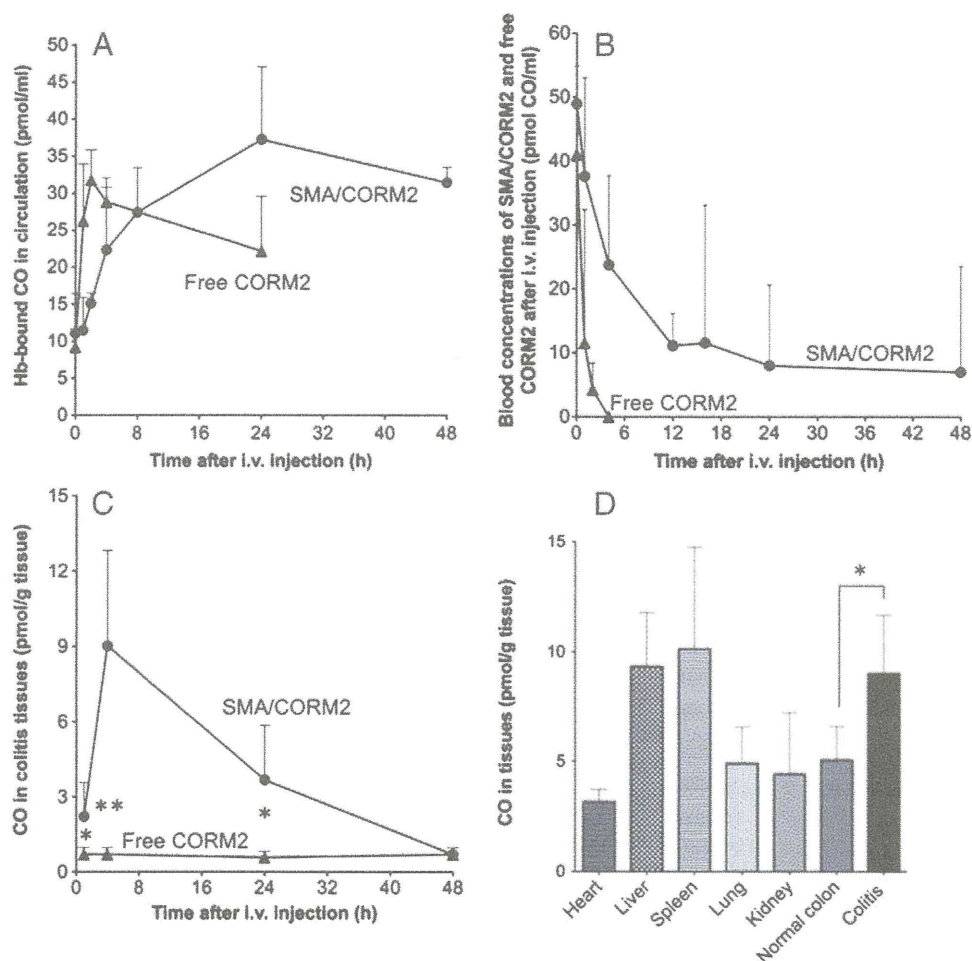


Fig. 3. *In vivo* pharmacokinetics of SMA/CORM2. (A) After i.v. administration of SMA/CORM2 or free CORM2 in healthy BALB/c mice, CO in circulation (mostly bound to hemoglobin) was measured by means of NOC7 to liberate CO, and the results were quantified by using gas chromatography. (B) The total CO, which included both hemoglobin-bound CO and CO derived from circulating SMA/CORM2 micelles, was quantified similarly but after using saponin. The net difference between the total CO and the hemoglobin-bound CO was utilized to evaluate the kinetics of SMA/CORM2 and free CORM2 in blood. After i.v. injection of SMA/CORM2 or free CORM2 to mice with DSS-induced colitis, CO concentrations in colonic tissues with colitis and in normal tissues were measured by using the same saponin method. (C) Time course of the CO concentrations in colitis tissues. (D) CO concentrations in each tissue including colitis tissues at 4 h after i.v. injection of SMA/CORM2. Data are means \pm SD; $n = 4-8$. * $p < 0.05$, ** $p < 0.01$. See text for details.

471 whereas the colon length improved markedly after SMA/CORM2
472 treatment; no significant difference in colon length was observed
473 between SMA/CORM2-treated mice and normal mice (Fig. 4C). The pro-
474 tective or therapeutic effect of SMA/CORM2 on colitis was also
475 supported by histological examination of colon tissues in each group.
476 Fig. 4D illustrates the tissue damage (e.g. necrosis and ulcers, as indicat-
477 ed by arrows) found in mice with DSS-induced colitis, whereas mice
478 treated with SMA/CORM2 had much less tissue damage and a histologi-
479 cal appearance that was similar to that of normal mice. These findings
480 clearly suggest the therapeutic potential of SMA/CORM2 for inflamma-
481 tory colitis.

482 SMA/CORM2 was also administered 3 days after DSS treatment,
483 when symptoms of colitis appeared, which is a reasonable protocol for
484 SMA/CORM2 as a therapeutic drug and a preventive agent. More impor-
485 tantly, SMA/CORM2 was administered only once, after which a

11.1 **Table 1**
11.2 Pharmacokinetic parameters of SMA/CORM2 and free CORM2.

11.3 Agent	$t_{1/2}$ (h) ^a	AUC ^b ($\mu\text{g}/\text{ml}/\text{h}$)	Total body clearance (L/h/kg)
11.4 CORM2	0.6	10.3	967.6
11.5 SMA/CORM2	23.2	171.2	58.9

11.6 ^a Plasma $t_{1/2}$ required to reach half-concentration at time zero by interpolation.

11.7 ^b Area under the plasma concentration vs. time curve.

486 significant therapeutic effect was achieved, and this effect was main-
487 tained for at least 3–4 days (Fig. 4A and B). These results thus support
488 the superior *in vivo* pharmacokinetics of SMA/CORM2, i.e. prolonged
489 CO bioavailability and circulation time of SMA/CORM2 (Fig. 3A and B),
490 which also strongly suggest the advantage of SMA-CORM2 compared
491 with free CORM2. In a previous report, Takagi et al. examined the effect
492 of free CORM2, applied twice daily during the experiment, on DSS-
493 induced colitis and found that the pathological changes of colitis tended
494 to improve, but these trends were less significant [10]. The advantages of
495 SMA/CORM2 compared with free CORM2, e.g. water solubility, slow and
496 constant release of CO, and improved pharmacokinetics, will thus great-
497 ly strengthen its therapeutic applicability, not only because of its in-
498 creased therapeutic effect but also because of better patient compliance.

499 In addition, as we expected, oral application of SMA/CORM2 pro-
500 duced therapeutic effects that were similar to those of the i.v. route
501 (Fig. 4), because of their similar pharmacokinetics of CO generation
502 *in vivo* especially the local CO production in colitis tissues (Supple-
503 mental data Fig. S3A, C). These results also indirectly supported the
504 pH stability of SMA/CORM2, and SMA/CORM2 should thus maintain
505 micellar stability while traveling through the stomach and entering
506 the intestine. We recently reported that SMA micelles were more
507 quickly taken up by cells compared with other polymeric micelles
508 such as pegylated compounds [30]. Also, during their internalization,
509 micelles may partly undergo disintegration in the cell membrane, as
509

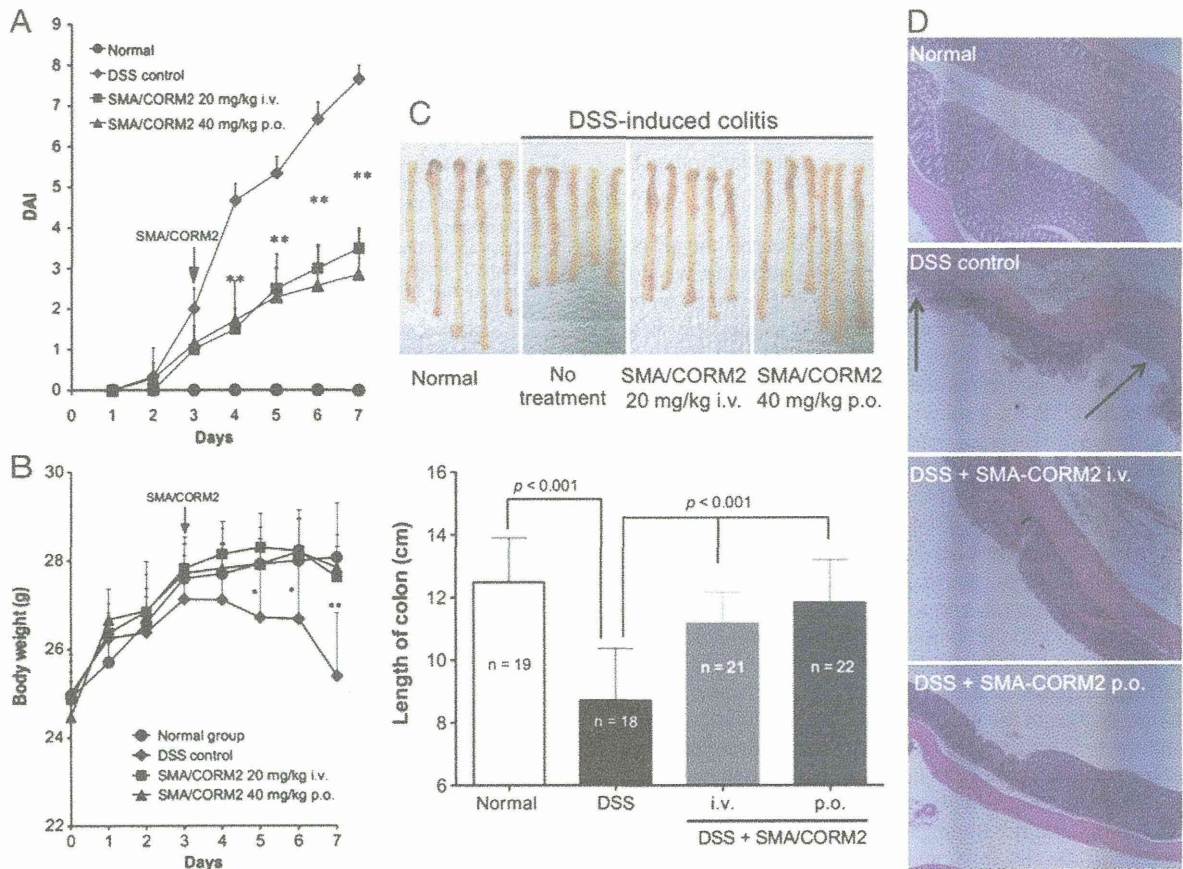


Fig. 4. Therapeutic effect of SMA/CORM2 on DSS-induced murine colitis. The DSS-induced colitis model was established by oral administration of 2% DSS for 1 week. During the experiments, colitis symptoms were recorded daily to obtain the DAI values. On day 3, when colitis symptoms appeared, SMA/CORM2 was administered i.v. or orally (p.o.). On day 7, when severe colitis appeared, mice were killed, the length of the colon was measured, and histological examination of the colon was performed. (A and B) Daily changes in DAI values and body weights of the mice, respectively. (C) Length of the colon of mice with or without SMA/CORM2 treatment. (D) Histology of the colon tissues of different groups after H&E staining. Arrows indicate necrosis and ulcers in the mucosa of the colon. See text for details. Values are means \pm SD; n = 18–22; *p < 0.05, **p < 0.01, SMA/CORM2 treatment group vs. DSS-induced colitis group.

510 shown by the lecithin-related release of CO (Fig. 2A). This may be
 511 included in the mechanisms by which SMA/CORM2 produces its ther-
 512 apeutic effect via the oral route. Namely, while SMA/CORM2

micelles may enter the circulation through the intestine to exert
 therapeutic effect systemically, some may exhibit therapeutic effect
 locally against colitis.

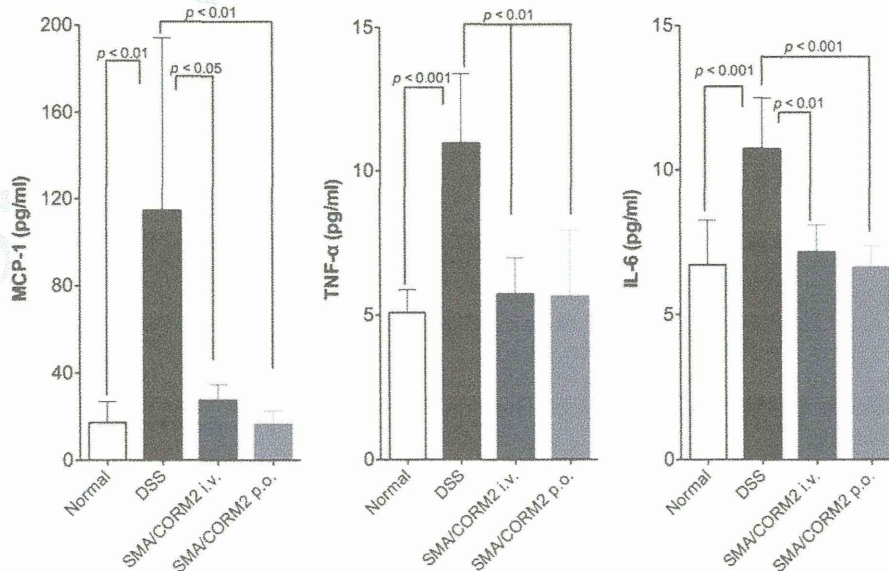


Fig. 5. Suppression of inflammatory cytokines (MCP-1, TNF- α , and IL-6) by SMA/CORM2 in DSS-induced murine colitis. The experimental protocol is the same as that described for Fig. 4. On day 7 of the experiment, mice were killed and serum samples were collected for measurement of the cytokines by using ELISA. Values are means \pm SD; n = 6–8. See text for details.

3.5. SMA/CORM2-induced suppression of the production of inflammatory cytokines in DSS-induced murine colitis

DSS-induced colitis, as an inflammatory disease, involves the generation of various inflammatory cytokines. In the present study, we also found increased serum levels of MCP-1, TNF- α , and IL-6 in mice receiving DSS (Fig. 5). SMA/CORM2 treatment significantly suppressed these cytokine levels to almost normal levels (Fig. 5). These findings are consistent with the improved symptoms and pathology of colitis after treatment with SMA/CORM2, as Fig. 4 shows.

Many researchers have reported potent anti-inflammatory effects of CO [31], including reduced production of inflammatory mediators in macrophages after various stimuli such as bacterial endotoxin, cytokines, and hypoxia-reoxygenation [32–34], and decreased levels of proinflammatory proteins such as inducible NO synthase, cyclooxygenase 2, and prostaglandins [35]. In addition, the major producers of inflammatory cytokines—infilitrated neutrophils and activated macrophages [36,37]—are the main sources of ROS in inflammatory diseases, which suggests the involvement of ROS in the inflammatory process. Bulua et al. recently reported that ROS are crucial for bacterial endotoxin-stimulated macrophages for the production of several proinflammatory cytokines, which is an essential feature of innate immunity [38]. CORM2 also reportedly had tissue protective effects against ischemia–reperfusion injury of the liver, which is a widely known ROS-related disease [9]. These data, both previous reports and the findings described here in this study, therefore suggest that the anti-inflammatory and anti-oxidative effects of CO are probably the major mechanisms involved in the therapeutic activity of SMA/CORM2 in inflammatory colitis.

4. Conclusions

We successfully prepared a water-soluble micellar CO donor, SMA/CORM2, by using the biocompatible amphiphilic polymer SMA. In addition to much improved water solubility, these micelles exhibited sustained and slow CO release, as well as superior *in vivo* pharmacokinetics, *i.e.* prolonged $t_{1/2}$ in circulation and selective accumulation in inflammatory tissues. In our DSS-induced murine colitis model, SMA/CORM2 showed marked therapeutic and tissue protective effects, probably through CO released from the micelles, which produced anti-oxidative and anti-inflammatory effects. We thus anticipate that SMA/CORM2 micelles can be applied to the treatment of IBD as well as other ROS-related inflammatory diseases including ischemia–reperfusion injury, bacterial and viral infections, and hypertension, and thus further investigations of these SMA/CORM2 micelles are warranted.

Acknowledgments

This work was supported in part by Grants-in-Aid for Scientific Research on Cancer Priority Areas (20015045) and Scientific Research (C) (20590049 and S0801085) from the Ministry of Education, Culture, Sports, Science and Technology of Japan, and by a grant from the Ministry of Health, Welfare and Labour (No. 23000001, H 23 3rd Cancer Study Project of Japan) to H.M. and J.F.

Appendix A. Supplementary data

Supplementary data to this article can be found online at <http://dx.doi.org/10.1016/j.jconrel.2014.05.018>.

References

- [1] R. Motterlini, L.E. Otterbein, The therapeutic potential of carbon monoxide, *Nat. Rev. Drug Discov.* 9 (2010) 728–743, <http://dx.doi.org/10.1038/nrd3228>.
- [2] N.G. Abraham, A. Kappas, Pharmacological and clinical aspects of heme oxygenase, *Pharmacol. Rev.* 60 (2008) 79–127, <http://dx.doi.org/10.1124/pr.107.07104>.

- [3] P.A. Rodgers, H.J. Vreman, P.A. Dennery, D.K. Stevenson, Sources of carbon monoxide (CO) in biological systems and applications of CO detection technologies, *Semin. Perinatol.* 18 (1994) 2–10.
- [4] M.D. Maines, Heme oxygenase: function, multiplicity, regulatory mechanisms, and clinical applications, *FASEB J.* 2 (1988) 2557–2568.
- [5] J. Fang, T. Akaike, H. Maeda, Antiapoptotic role of heme oxygenase (HO) and the potential of HO as a target in anticancer treatment, *Apoptosis* 9 (2004) 27–35.
- [6] S. Tanaka, T. Akaike, J. Fang, T. Beppu, M. Ogawa, F. Tamura, Y. Miyamoto, H. Maeda, Antiapoptotic effect of haem oxygenase-1 induced by nitric oxide in experimental solid tumour, *Br. J. Cancer* 88 (2003) 902–909.
- [7] J. Fang, H. Qin, T. Seki, H. Nakamura, K. Tsukigawa, T. Shin, H. Maeda, Therapeutic potential of pegylated hemin for reactive oxygen species-related diseases via induction of heme oxygenase-1: results from a rat hepatic ischemia/reperfusion injury model, *J. Pharmacol. Exp. Ther.* 339 (2011) 779–789, <http://dx.doi.org/10.1124/jpet.111.185348>.
- [8] D.E. Baranano, M. Rao, C.D. Ferris, S.H. Snyder, Biliverdin reductase: a major physiological cytoprotectant, *Proc. Natl. Acad. Sci. U. S. A.* 99 (2002) 16093–16098.
- [9] Y. Wei, P. Chen, M. de Bruyn, W. Zhang, E. Bremer, W. Helfrich, Carbon monoxide-releasing molecule-2 (CORM-2) attenuates acute hepatic ischemia reperfusion injury in rats, *BMC Gastroenterol.* 10 (2010) 42, <http://dx.doi.org/10.1186/1471-230X-10-42>.
- [10] T. Takagi, Y. Naito, K. Uchiyama, T. Suzuki, I. Hirata, K. Mizushima, H. Tsuboi, N. Hayashi, O. Handa, T. Ishikawa, N. Yagi, S. Kokura, H. Ichikawa, T. Yoshikawa, Carbon monoxide liberated from carbon monoxide-releasing molecule exerts an anti-inflammatory effect on dextran sulfate sodium-induced colitis in mice, *Dig. Dis. Sci.* 56 (2011) 1663–1671, <http://dx.doi.org/10.1007/s10620-010-1484-y>.
- [11] R. Motterlini, Carbon monoxide-releasing molecules (CO-RMs): vasodilatory, anti-ischaemic and anti-inflammatory activities, *Biochem. Soc. Trans.* 35 (2007) 1142–1146.
- [12] H. Maeda, Vascular permeability in cancer and infection as related to macromolecular drug delivery, with emphasis on the EPR effect for tumor-selective drug targeting, *Proc. Jpn. Acad. Ser. B Phys. Biol. Sci.* 88 (2012) 53–71.
- [13] Y. Matsumura, H. Maeda, A new concept for macromolecular therapeutics in cancer chemotherapy: mechanism of tumorotropic accumulation of proteins and the anti-tumor agent smancs, *Cancer Res.* 46 (1986) 6387–6392.
- [14] H. Maeda, Macromolecular therapeutics in cancer treatment: the EPR effect and beyond, *J. Control. Release* 164 (2012) 138–144, <http://dx.doi.org/10.1016/j.jconrel.2012.04.038>.
- [15] J. Fang, H. Nakamura, H. Maeda, The EPR effect: unique features of tumor blood vessels for drug delivery, factors involved, and limitations and augmentation of the effect, *Adv. Drug Deliv. Rev.* 63 (2011) 136–151, <http://dx.doi.org/10.1016/j.addr.2010.04.009>.
- [16] D.C. Baumgart, S.R. Carding, Inflammatory bowel disease: cause and immunobiology, *Lancet* 369 (2007) 1627–1640.
- [17] B. Khor, A. Gardet, R.J. Xavier, Genetics and pathogenesis of inflammatory bowel disease, *Nature* 474 (2011) 307–317, <http://dx.doi.org/10.1038/nature10209>.
- [18] T. Ohkusa, T. Nomura, N. Sato, The role of bacterial infection in the pathogenesis of inflammatory bowel disease, *Intern. Med.* 43 (2004) 534–539.
- [19] J.C. Arthur, E. Perez-Chanona, M. Mühlbauer, S. Tomkovich, J.M. Uronis, T.J. Fan, B.J. Campbell, T. Abujamel, B. Dogan, A.B. Rogers, J.M. Rhodes, A. Stintzi, K.W. Simpson, J.J. Hansen, T.O. Keku, A.A. Fodor, C. Jobin, Intestinal inflammation targets cancer-inducing activity of the microbiota, *Science* 338 (2012) 120–123, <http://dx.doi.org/10.1126/science.1224820>.
- [20] A. Rezaie, R.D. Parker, M. Abdollahi, Oxidative stress and pathogenesis of inflammatory bowel disease: an epiphenomenon or the cause? *Dig. Dis. Sci.* 52 (2007) 2015–2021.
- [21] K.P. Pavlick, F.S. Laroux, J. Fuseler, R.E. Wolf, L. Gray, J. Hoffman, M.B. Grisham, Role of reactive metabolites of oxygen and nitrogen in inflammatory bowel disease, *Free Radic. Biol. Med.* 33 (2002) 311–322.
- [22] A.K. Iyer, K. Greish, J. Fang, R. Murakami, H. Maeda, High-loading nanosized micelles of copoly(styrene-maleic acid)-zinc protoporphyrin for targeted delivery of a potent heme oxygenase inhibitor, *Biomaterials* 28 (2007) 1871–1881.
- [23] A.M. Sundin, J.E. Larsson, Rapid and sensitive method for the analysis of carbon monoxide in blood using gas chromatography with flame ionisation detection, *J. Chromatogr. B Anal. Technol. Biomed. Life Sci.* 766 (2002) 115–121.
- [24] S. Wirtz, C. Neufert, B. Weigmann, M.F. Neurath, Chemically induced mouse models of intestinal inflammation, *Nat. Protoc.* 2 (2007) 541–546.
- [25] K. Greish, T. Sawa, J. Fang, T. Akaike, H. Maeda, SMA-doxorubicin, a new polymeric micellar drug for effective targeting to solid tumours, *J. Control. Release* 97 (2004) 219–230.
- [26] R. Duncan, Polymer therapeutics as nanomedicines: new perspectives, *Curr. Opin. Biotechnol.* 22 (2011) 492–501, <http://dx.doi.org/10.1016/j.copbio.2011.05.507>.
- [27] R. Duncan, M.J. Vicent, Polymer therapeutics—prospects for 21st century: the end of the beginning, *Adv. Drug Deliv. Rev.* 65 (2013) 60–70, <http://dx.doi.org/10.1016/j.addr.2012.08.012>.
- [28] J. Cassidy, D.R. Newell, S.R. Wedge, J. Cummings, Pharmacokinetics of high molecular weight agents, *Cancer Surv.* 17 (1993) 315–341.
- [29] N. Nishiyama, K. Kataoka, Current state, achievements, and future prospects of polymeric micelles as nanocarriers for drug and gene delivery, *Pharmacol. Ther.* 112 (2006) 630–648.
- [30] H. Nakamura, J. Fang, B. Gabininath, K. Tsukigawa, H. Maeda, Intracellular uptake and behavior of two types zinc protoporphyrin (ZnPP) micelles, SMA-ZnPP and PEG-ZnPP as anticancer agents: unique intracellular disintegration of SMA micelles, *J. Control. Release* 155 (2011) 367–375, <http://dx.doi.org/10.1016/j.jconrel.2011.04.025>.

- 658 [31] R. Motterlini, L.E. Otterbein, The therapeutic potential of carbon monoxide, *Nat. Rev.*
659 *Drug Discov.* 9 (2010) 728–743, <http://dx.doi.org/10.1038/nrd3228>.
- 660 [32] L.E. Otterbein, F.H. Bach, J. Alam, M. Soares, H. Tao Lu, M. Wysik, R.J. Davis, R.A. Flavell,
661 A.M. Choi, Carbon monoxide has anti-inflammatory effects involving the mitogen-
662 activated protein kinase pathway, *Nat. Med.* 6 (2000) 422–428.
- 663 [33] P. Sawle, R. Foresti, B.E. Mann, T.R. Johnson, C.J. Green, R. Motterlini, Carbon
664 monoxide-releasing molecules (CO-RMs) attenuate the inflammatory response
665 elicited by lipopolysaccharide in RAW264.7 murine macrophages, *Br. J. Pharmacol.*
666 145 (2005) 800–810.
- 667 [34] M.G. Bani-Hani, D. Greenstein, B.E. Mann, C.J. Green, R. Motterlini, Modulation of
668 thrombin-induced neuroinflammation in BV-2 microglia by carbon monoxide-
669 releasing molecule 3, *J. Pharmacol. Exp. Ther.* 318 (2006) 1315–1322.
- [35] K. Tsoyi, Y.M. Ha, Y.M. Kim, Y.S. Lee, H.J. Kim, H.J. Kim, H.G. Seo, J.H. Lee, K.C. Chang, 670
671 Activation of PPAR- γ by carbon monoxide from CORM-2 leads to the inhibition of
672 iNOS but not COX-2 expression in LPS-stimulated macrophages, *Inflammation* 32
673 (2009) 364–371, <http://dx.doi.org/10.1007/s10753-009-9144-0>.
- [36] C. Nathan, Neutrophils and immunity: challenges and opportunities, *Nat. Rev.* 674
Immunol. 6 (2006) 173–182. 675
- [37] D.M. Mosser, J.P. Edwards, Exploring the full spectrum of macrophage activation, 676
Nat. Rev. Immunol. 8 (2008) 958–969, <http://dx.doi.org/10.1038/nri2448>. 677
- [38] A.C. Butua, A. Simon, R. Maddipati, M. Pelletier, H. Park, K.Y. Kim, M.N. Sack, D.L. 678
679 Kastner, R.M. Siegel, Mitochondrial reactive oxygen species promote production of
680 proinflammatory cytokines and are elevated in TNFR1-associated periodic syndrome
681 (TRAPS), *J. Exp. Med.* 208 (2011) 519–533, <http://dx.doi.org/10.1084/jem.20102049>.

682

UNCORRECTED PROOF

Running title: Failure of chemotherapy: Needs for tumor selective drug delivery

Review article for *Proc. Jpn. Academy Ser. B*

Analysis of the causes of failures in cancer chemotherapy and
improvements for tumor-selective drug delivery, therapeutic
efficacy, and eliminating adverse effects

Hiroshi Maeda

Institute of Drug Delivery Science

Sojo University

Kumamoto, Japan

Communicated by: Takashi Sugimura, a member of Japan Academy

Corresponding Author: Hiroshi Maeda, Professor, Research Institute for Drug Delivery
Science, Sojo University, Ikeda 4-22-1, Nishi-ku, Kumamoto, 860-0082, Japan.

E-mail address: hirmaeda@ph.sojo-u.ac.jp

Tel.: +81-96-326-4114; Fax: +81-96-326-3185

Total word count:

Word count of the abstract:

Contents

Abstract.....	3
1. Introduction	4
1-1. Background.....	4
1-2. Analyses of chemotherapeutic failures.....	5
1-2-1. Indiscriminate drug distribution to normal tissues and tumors, with no tumor-selective drug delivery.....	5
1-2-2. Genetic diversity or heterogeneity.....	6
1-2-3. Immunotherapy: still not decisive weaponry against cancer.....	7
1-2-4. Issues related to the stability of liposomal and micellar drugs in relation to the EPR effect and tumor accumulation.....	8
1-2-5. Problems in cancer drug screening and evaluation.....	12
1-2-6. Problems in photodynamic therapy.....	15
1-2-7. Adverse effects of cancer chemotherapy.....	17
1-2-8. Economic issues: poor response rates, prohibitive costs, and problems with the health insurance system.....	17
2. Solutions to tumor-selective drug development: The EPR effect and sound rationales for drug design.....	19
3. Problems with the EPR effect for tumor-selective drug delivery.....	21
4. Augmentation of the EPR effect for tumor delivery.....	26
5. The EPR effect in metastatic cancer and outlook for polymer-conjugated candidate drug 1.....	27
6. Photodynamic therapy (PDT) using macromolecular candidate drug 2	31
7. Conclusion.....	34

Abstract

Cancer chemotherapy for solid tumors has had limited success. Despite enthusiasm about molecular target and antibody drugs, cancer vaccines, and “missile therapy” with incredible prices, retrospective evaluations revealed disappointing outcomes. This review discusses causes of these unsuccessful modalities, conventional drugs, photodynamic therapy, and problems with drug-screening models. One cause may be attributed to extensive genetic polymorphism in human solid tumors. Also, few therapeutic modalities fully utilized universal or common characteristics of solid cancers. We investigated the more universal component of solid tumors—vasculature and neovasculature. Solid tumors have a unique vascular architecture and hyperproduction of vascular mediators such as nitric oxide and bradykinin. Our tumor-selective drug delivery utilizes the mechanism based on the enhanced permeability and retention (EPR) effect of macromolecular drugs, a unique feature of solid tumors. The characteristics of the EPR effect can improve tumor-selective macromolecular drug delivery, followed by release of active principle because of the low pH in solid tumors, and can thus improve therapeutic outcome.

Keywords: cancer chemotherapy, cause of failure, EPR effect, molecular target drugs, drug design, health care cost

Abbreviations

MW: molecular weight; ROS: reactive oxygen species; VEGF: vascular endothelial growth factor; EGF: epidermal growth factor; PEG: polyethylene glycol; EPR: enhanced permeability and retention; DOX: doxorubicin; i.v.: intravenous; THP: tetrahydropyranyl; ZnPP: zinc protoporphyrin; HPMA: *N*-(2-hydroxypropyl)methacrylamide; SMA: styrene-co-maleic acid; NCS: neocarzinostatin; NO₂⁻: nitrite; NO: nitric oxide; P-THP: polymer-conjugated

pirarubicin; P-ZnPP: polymer-conjugated zinc protoporphyrin; PDT: photodynamic therapy

1. Introduction

1-1. Background. Reviewing 60 years of the history of cancer chemotherapy reveals only limited success for treatment of leukemia and non-solid tumors. In the past few decades, tumor-targeting (or "missile") therapy, such as molecular target drugs (*e.g.*, for specific receptors or kinases), antibody conjugates, cancer vaccines, and advanced technology-based nanomedicines, in addition to many conventional drugs of low molecular weight (MW), have been developed to treat various cancers. However, when patients have stage III or IV disease, as is the case for most cancer patients seen in clinical settings, they usually have metastatic cancers that most frequently affect the lymph nodes, liver, lungs, bones, and brain, as well as other organs. Furthermore, many cancers develop resistance to multiple drugs and fail to respond effectively to these drugs¹⁾. Therefore, at these stages of disease, therapeutic modalities are quite limited. In addition, in recent years several extensive trials of vaccines against prostate, lung, pancreatic, and skin cancers all failed to produce positive results. Despite these